Paper 45

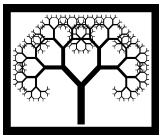

Proceedings of the Eighth International Conference
on Engineering Computational Technology,
B.H.V. Topping, (Editor),
Civil-Comp Press, Stirlingshire, Scotland

Singularities in Isogeometric Analysis

T. Takacs
Institute of Applied Geometry
Johannes Kepler University, Linz, Austria

Abstract

Isogeometric analysis is a method which directly uses the NURBS based representation from computer aided design for numerical simulation. We analyse the influence of singularities in the parametrisation of the physical domain. If singularities occur the test function spaces from isogeometric analysis might not fulfill the desired regularity properties. We present regularity results for various singularly parametrised domains, like triangles and fillets, and a modification scheme to regain regularity for those cases. In addition we present local refinement strategies that lead to geometrically regular splittings of singular patches. We also discuss the influence of inner control points on the regularity of the test function space.

Keywords: isogeometric analysis, computer aided design, singularity, parametrisation, regularity, refinement.

1 Introduction

Isogeometric analysis was introduced by Hughes and his group in 2005 [13]. It was a major step forward in unifying the worlds of computer aided design (CAD) and computer aided engineering (CAE). Historically, both fields developed separately and are based on different methods for different objects and primitives. Isogeometric analysis is a numerical simulation method that incorporates the non-uniform rational B-spline (NURBS) based representation of CAD models into a physical or engineering problem. The underlying physical domain as a part of the 2- or 3-dimensional space is parametrised by 2- or 3-variate NURBS. To describe the physical problem one has to set up a proper function space on the physical domain. In isogeometric analysis this function space is derived from the NURBS parametrisation. Therefore the properties of the function space are induced by properties of the parametrisation. Hence, finding

"good" parametrisations is an important task (see e.g. [17, 5]).

If the parametrisation is assumed to be regular, then the tensor product structure of multivariate NURBS leads to domains that are structurally equivalent to a quadrangle or to a hexahedron. Hence this straightforward approach cannot be used to parametrise more complex shapes. There are several strategies to cope with this problem. One possibility is to split the domain into regularly parametrised quadrangular or hexahedral parts [6, 16]. Following this procedure one has to take care of the thus created inner boundaries. This procedure leads to separate function spaces on each part of the splitting. Depending on the imposed continuity of the problem these function spaces have to be connected and restricted properly. This task can be very costly. Another strategy is to use trimmed patches [12, 15]. Applying this method allows to represent very general domains. But the trimming may result in function spaces with poor stability properties. A different approach is to use singular parametrisations [18, 19]. Singularly parametrised surfaces and volumes can represent non-quadrangular or non-hexahedral domains in one piece. In that case splitting or trimming of the domain is not necessary. Hence singular parametrisations can be very convenient.

In this paper we focus on domains that are parametrised by singular mappings. We examine properties of the singularities and analyse how they influence the function spaces. We give an overview of the regularity results on singularly parametrised domains. From these results we deduce parametrisation strategies depending on the physical problem and on the shape of the domain. A test function on the physical domain is defined as the composition of a basis function on the parameter space with the inverse of the parametrisation. Since the parametrisation is assumed to have singularities the inverse and its derivatives are not well defined in these singular points. This leads to test functions that do not fulfill the desired regularity and differentiability conditions. Consequently, numerical methods to solve partial differential equations cannot be applied properly.

First we discuss the regularity properties of the test function space. We consider several types of singularities of B-spline parametrisations for 2-dimensional domains. Different types of singularities are used to represent different geometric properties of the physical domain. For the considered types of singularities we show regularity properties of the test function space. In addition we derive modification schemes for the test function space in case of insufficient regularity.

Another focus of our work lies on the regularity of the polynomial patches after refinement. In the presence of singularities some of the patches might degenerate. We analyse this behaviour for different types of singularities. These results are crucial for the numerical analysis of solution methods for physical problems.

2 Preliminaries

In this section we present in short the notion of isogeometric analysis as a method for the solution of partial differential equations. We recall the basic definitions of

isogeometric analysis (see [13]) and the goals of this paper.

2.1 Representation of the geometry of the domain

In isogeometric analysis the physical domain is represented by a B-spline or NURBS parametrisation. In this paper we restrict ourselves to B-splines. Note that many of the results can be generalized to NURBS parametrisations fulfilling certain additional conditions (see [24]). We start with the definition of B-splines, which are piecewise polynomial functions determined by some degree $d \in \mathbb{Z}_0^+$ and a knot vector $\mathrm{T} = (t_0, \ldots, t_{m-1})$; a non-decreasing sequence of real numbers. We assume that the knot vector is open, i.e. the first and last knot is repeated $d+1$ times. For $i = 0, \ldots, m-d-2$ the i-th B-spline $b_{i,d}$ of degree d is defined by the recurrence

$$\begin{aligned} b_{i,0}(x) &= \begin{cases} 1 & \text{for } t_i \le x \le t_{i+1} \\ 0 & \text{else} \end{cases} \\ b_{i,d}(x) &= \frac{x - t_i}{t_{i+d} - t_i} b_{i,d-1}(x) + \frac{t_{i+d+1} - x}{t_{i+d+1} - t_{i+1}} b_{i+1,d-1}(x), \end{aligned}$$

where all fractions with a zero denominator are considered to be equal to zero. The parameter space is set to be $\mathrm{B} =]t_d, t_{m-d-1}[$, which covers the support of all the B-splines, except for the boundary points $t_0 = \ldots = t_d$ and $t_{m-d-1} = \ldots = t_{m-1}$.

To extend the definition of B-splines to higher dimensions we recall the concept of tensor product B-splines. Consequently, a degree and a knot vector is set for each direction. Here we consider bivariate B-splines only ($n = 2$). We have given a degree $\mathbf{d} = (d_1, d_2)$ and a knot vector $\mathbf{T} = \left(\mathrm{T}^{(1)}, \mathrm{T}^{(2)}\right)$, with $\mathrm{T}^{(1)} \in \mathbb{R}^{m_1}$ and $\mathrm{T}^{(2)} \in \mathbb{R}^{m_2}$. Using the notation $\mathbf{i} = (i, j)$ and $\mathbf{x} = (x, y)^T$, the $\mathbf{i}$-th bivariate B-spline of degree $\mathbf{d}$ and knot vector $\mathbf{T}$ is defined by

$$\begin{aligned} b_{\mathbf{i},\mathbf{d}} : \mathbf{B} &\to \mathbb{R} \\ \mathbf{x} &\mapsto b_{i,d_1}(x)\, b_{j,d_2}(y), \end{aligned}$$

for $\mathbf{0} \le \mathbf{i} \le \mathbf{m} - \mathbf{d} - \mathbf{2}$. Here b_{i,d_ℓ} is the i-th B-spline corresponding to d_ℓ and $\mathrm{T}^{(\ell)}$ for $\ell = 1, 2$. The parameter space $\mathbf{B}$ is defined by

$$\mathbf{B} = \left]t_{d_1}^{(1)}, t_{m_1-d_1-1}^{(1)}\right[\times \left]t_{d_2}^{(2)}, t_{m_2-d_2-1}^{(2)}\right[.$$

For a more detailled information on B-splines see [21, 22, 20].

Without loss of generality we set the parameter space to be the 2-dimensional open unit box $\mathbf{B} =]0, 1[^2$. We assume the degree $\mathbf{d}$ to be fixed. To simplify the notation we omit the subscript $\mathbf{d}$ and write $b_{\mathbf{i}}$. For a given (initial) knot vector $\mathbf{T}$ the parametrisation $\mathbf{G}$ of Ω is defined by

$$\begin{aligned} \mathbf{G} : \mathbf{B} &\to \mathbb{R}^2 \\ \mathbf{x} &\mapsto \sum_{\mathbf{i} \in \mathbb{I}_\circ} \mathbf{P}_{\mathbf{i}} b_{\mathbf{i}}(\mathbf{x}), \end{aligned}$$

with B-spline basis functions $b_{\mathbf{i}}$ and control points $\mathbf{P}_{\mathbf{i}} \in \mathbb{R}^2$ for each

$$\mathbf{i} \in \mathbb{I}_\circ = \left\{ \mathbf{i} \in \mathbb{Z}^2 : \mathbf{0} \leq \mathbf{i} \leq \mathbf{m} - \mathbf{d} - \mathbf{2} \right\}.$$

The physical domain $\Omega \subset \mathbb{R}^2$ is the image of $\mathbf{B}$ under $\mathbf{G}$, i.e. $\mathbf{G}(\mathbf{B}) = \Omega$. We assume that the parametrisation $\mathbf{G}$ is bijective in the interior of the parameter space. In practical applications it might happen that overlaps occur in the geometry mapping. In that case the parametrisation is not bijective. Note that we will not consider this kind of parametrisations.

2.2 The numerical method

We have given an 2-dimensional physical domain $\Omega \subseteq \mathbb{R}^2$ parametrised by the function $\mathbf{G} : \mathbf{B} \to \mathbb{R}^2$. One might want to solve some differential equation on this domain. The differentail equation often derives from a physical problem; like stress analysis, flow simulation, fluid structure interaction or electromagnetics (see e.g. [26, 4, 14, 7]). The differential equation can be transformed to a variational formulation as in Model Problem 2.1. In this section we look at the definition of such a variational problem and recall the isogeometric method to solve this kind of problems. Concerning the numerical background we refer to [3].

Let $\mathcal{V}_g(\Omega), \mathcal{V}_0(\Omega) \subseteq \mathcal{V}(\Omega)$ be subsets of the Hilbert space $\mathcal{V}(\Omega)$; where $\mathcal{V} = H^1$ or $\mathcal{V} = H^2$, with

$$H^1(\Omega) = \left\{ \varphi(\boldsymbol{\xi}) \in L^2(\Omega) : \frac{\partial \varphi}{\partial \xi_k} \in L^2(\Omega) \; \forall \, 1 \leq k \leq 2 \right\}$$

and

$$H^2(\Omega) = \left\{ \varphi(\boldsymbol{\xi}) \in H^1(\Omega) : \frac{\partial^2 \varphi}{\partial \xi_k \partial \xi_l} \in L^2(\Omega) \; \forall \, 1 \leq l, k \leq 2 \right\}.$$

Given a bilinear form $\alpha(\cdot,\cdot) : \mathcal{V}_g \times \mathcal{V}_0 \to \mathbb{R}$ and a linear functional $\langle \lambda, \cdot \rangle : \mathcal{V}_0 \to \mathbb{R}$ we consider a variational formulation of a partial differential equation.

Model Problem 2.1 (Variational problem) *Find* $\varphi \in \mathcal{V}_g(\Omega)$ *such that*

$$\alpha(\varphi, \psi) = \langle \lambda, \psi \rangle \qquad \forall \; \psi \in \mathcal{V}_0(\Omega).$$

The isogeometric method is an approach to discretize such a variational problem. It is based on Galerkin's principle, which can be interpreted in the following way. We have given a sequence $\{\mathcal{V}_h\}_h$ of finite-dimensional function spaces $\mathcal{V}_h \subseteq \mathcal{V}$. Here h can be seen as the mesh size of the discretization of the domain. In the limit case $h \to 0$ the solution of the discrete problem 2.2 should converge to the solution of the continuous problem 2.1. Spaces $\mathcal{V}_{g,h} = \mathcal{V}_g \cap \mathcal{V}_h$ and $\mathcal{V}_{0,h} = \mathcal{V}_0 \cap \mathcal{V}_h$ are set up to solve the following discrete problem for each h.

Model Problem 2.2 *Find* $\varphi_h \in \mathcal{V}_{g,h}(\Omega)$ *such that*

$$\alpha(\varphi_h, \psi_h) = \langle \lambda, \psi_h \rangle \qquad \forall \psi_h \in \mathcal{V}_{0,h}(\Omega).$$

In the setting of this paper the basis functions spanning $\mathcal{V}_h$ are constructed from the B-splines $b_{\mathbf{i}}$ and from the domain parametrisation $\mathbf{G}$. To set up a basis of $\mathcal{V}_h$ for decreasing mesh size h we first need to define the refinement scheme.

A family of meshes $\{\mathcal{D}_h\}_h$ is derived from a family of refined knot spans. Each mesh $\mathcal{D}_h$ is a partition of the box $\mathbf{B}$ into elements D. The partition may have a tensor product structure, but we might also consider a local refinement, as it appears in the context of THB-splines [11, 10], LR-splines [9] or T-splines [8, 1, 23]. Nonetheless, we will not go into the details of the various local refinement procedures here. We only introduce some notations for tensor product refinement. Each element $D \in \mathcal{D}_h$ is an open and non-empty 2-dimensional interval with diameter h_D, with $h = \max(h_D)$ for each partition $\mathcal{D}_h$. We set the h-dependent index space $\mathbb{I}_h$ to

$$\mathbb{I}_h = \left\{\mathbf{i} \in \mathbb{Z}^2 : \mathbf{0} \leq \mathbf{i} \leq \mathbf{m}_h - \mathbf{d} - \mathbf{2}\right\}.$$

We define

$$\mathcal{S}_h = \text{span}\left(\{b_{\mathbf{i},h} : \mathbf{i} \in \mathbb{I}_h\}\right)$$

as a function space on $\mathbf{B}$ and the space

$$\mathcal{V}_h = \text{span}\left(\{\beta_{\mathbf{i},h} : \mathbf{i} \in \mathbb{I}_h\}\right)$$

on Ω, with

$$\beta_{\mathbf{i},h} = b_{\mathbf{i},h} \circ \mathbf{G}^{-1} : \Omega \to \mathbb{R}.$$

To have well-defined functions $\beta_{\mathbf{i},h}$ we assume that the parametrisation $\mathbf{G}$ is invertible in the open box $\mathbf{B}$. Nonetheless it may be singular in some points $x_0 \in \bar{\mathbf{B}}$.

For each element $D \in \mathcal{D}_h$ we have $\Delta = \mathbf{G}(D) \subset \Omega$. Let Λ_h be the collection of all such Δ, let $\theta_\Delta = \text{diam}(\Delta)$ and $\theta = \max(\theta_\Delta)$. Hence h is the mesh size in the parameter domain and θ is the mesh size in the physical domain. Let ρ_Δ be the diameter of the largest inscribed circle of the patch Δ. Furtheron let $|\Delta|$ be the area of Δ. We say that the mesh is degenerating if there exist Δ such that the ratio $\theta_\Delta/\rho_\Delta$ is going to infinity as h tends to 0.

2.3 Regularity properties and refinement

In many practical applications it is desireable that the test function space $\mathcal{V}_h$ fulfills $\mathcal{V}_h \subseteq H^m$ for $m = 1, 2$. The study of harmonic or biharmonic equations leads to H^1 or H^2, respectively, as underlying function spaces for the variation problem.

In the following sections we analyse the test functions from isogeometric analysis in the presence of singularities in the parametrisation. It might happen that some of the test functions $\beta_{\mathbf{i},h}$ do not fulfill $\beta_{\mathbf{i},h} \in H^1$ or $\beta_{\mathbf{i},h} \in H^2$. We will point out such cases and present a modification scheme to handle this problem efficiently. Furtheron we present local refinement schemes for several singularly parametrised domains. The findings of this paper strongly indicate that the approximation properties stated in [2] can be generalized from regular to certain singular domains as well.

3 Singular parametrisations of triangular domains

In this section we present three different parametrisations for a triangular domain. We analyze the regularity properties for the case of H^1 and H^2 as underlying function spaces. The presented parametrisations are of low degree but the results are also valid for parametrisations of higher degree. The results presented in this paper are based on [24, 25].

The singularities of the presented Bézier patches fall into two different categories. For **Triangle A** one edge in the parameter domain degenerates to a single point in the physical domain. For **Triangle B1** and **Triangle B2** two adjacent edges in the parameter domain have a common tangent direction at the center point of one edge in the physical domain. We always set the singular point in the parameter domain as well as in the physical domain to be the origin. For Triangles A and B1 we consider Bézier patches of degree $(1, 1)$. Triangle B2 is a Bézier patch of degree $(2, 2)$.

- **Triangle A: Collapsing edge.** Let Ω_A be a Bézier patch having control points

$$\begin{array}{lll} \mathbf{P}_{(i,j)} & j=0 & j=1 \\ \hline i=0 & (0,0)^T & (0,0)^T \\ i=1 & (1,0)^T & (1,1)^T \end{array}$$

  where the parametrisation fulfills

$$\mathbf{G}_A = (x, xy)^T .$$

- **Triangle B1: Collinear edges (bilinear).** Let Ω_B be a Bézier patch having control points

$$\begin{array}{lll} \mathbf{P}_{(i,j)} & j=0 & j=1 \\ \hline i=0 & (0,0)^T & \left(\frac{1}{2},\frac{1}{2}\right)^T \\ i=1 & \left(-\frac{1}{2},-\frac{1}{2}\right)^T & \left(\frac{1}{2},-\frac{1}{2}\right)^T \end{array}$$

  where the parametrisation fulfills

$$\mathbf{G}_{B1} = \frac{1}{2}(-x+y+xy, -x+y-xy)^T .$$

- **Triangle B2: Collinear edges (biquadratic).** Let Ω_B be a Bézier patch having control points

$$\begin{array}{llll} \mathbf{P}_{(i,j)} & j=0 & j=1 & j=2 \\ \hline i=0 & (0,0)^T & (0,0)^T & \left(\frac{1}{2},\frac{1}{2}\right)^T \\ i=1 & (0,0)^T & \left(\frac{1}{8},-\frac{1}{8}\right)^T & \left(\frac{1}{2},0\right)^T \\ i=2 & \left(-\frac{1}{2},-\frac{1}{2}\right)^T & \left(0,-\frac{1}{2}\right)^T & \left(\frac{1}{2},-\frac{1}{2}\right)^T \end{array}$$

  where the parametrisation fulfills

$$\mathbf{G}_{B2} = \frac{1}{2}\left(-x^2+xy+x^2y+y^2-xy^2, -x^2-xy+x^2y+y^2-xy^2\right)^T .$$

The parametrisations of Triangle A and Triangle B1 are bilinear and the parametrisation of Triangle B2 is biquadratic. For each domain we allow arbitrary refinement and degree elevation leading to a subdivision $\mathcal{D}_h$ and an index set $\mathbb{I}_h$. Assume we are given a function space $\mathcal{V}_h$ derived from such a refinement. The indices $\mathbf{i} \in \mathbb{I}_h$ correspond to the refined test functions in a straightforward way.

Remark 3.1 *Note that any tensor-product B-spline surface can be split into Bézier patches. Therefore results for basis functions on Bézier patches can be extended to more general domains with B-spline representations.*

We will now state regularity results for the test function spaces for the three cases separately.

3.1 Triangle A: Collapsing edge

For this type of singular domain we get the following general result for arbitrarily refined meshes $\mathcal{D}_h$.

Theorem 3.2 *Consider the triangular domain Ω_A with parametrisation $\mathbf{G}_A$. Let $\mathbb{I}_h$ be the index set corresponding to an arbitrarily refined function space $\mathcal{V}_h$. We set*

$$\mathbb{D}_1 = \{(i,j) \in \mathbb{I}_h : i = 0\} \quad \textit{and} \quad \mathbb{D}_2 = \{(i,j) \in \mathbb{I}_h : i \leq 1\}.$$

The test functions $\beta_{\mathbf{i},h}$ fulfill $\beta_{\mathbf{i},h} \notin H^1(\Omega_A)$ if and only if $\mathbf{i} \in \mathbb{D}_1$. Moreover, they satisfy $\beta_{\mathbf{i},h} \notin H^2(\Omega_A)$ if and only if $\mathbf{i} \in \mathbb{D}_2$.

Proof. For a proof of this theorem see [24, 25]. □

Note that in this case the control points fulfill $P_{\mathbf{i}} = (0,0)^T$ for all $\mathbf{i} \in \mathbb{D}_1$.

This theorem states that, in the case of a singular parametrisation, some of the test functions are not sufficiently regular. In the next proposition we present a scheme to compute a basis for the space $\mathcal{V}_h \cap H^1(\Omega_A)$.

Proposition 3.3 *Let the assumptions and definitions of Theorem 3.2 be valid. For*

$$\hat{\beta}_{(0,0),h}(\boldsymbol{\xi}) = \sum_{\mathbf{i} \in \mathbb{D}_1} \beta_{\mathbf{i},h}(\boldsymbol{\xi})$$

and

$$\hat{\mathcal{V}}_h = \operatorname{span}\left(\left\{\hat{\beta}_{(0,0),h}\right\} \cup \{\beta_{\mathbf{i},h} : \mathbf{i} \in \mathbb{I}_h \backslash \mathbb{D}_1\}\right)$$

we have $\hat{\mathcal{V}}_h = \mathcal{V}_h \cap H^1(\Omega_A)$.

Proof. The statement follows directly from the proof of Proposition 3.7 which we present later. □

The basis

$$\left\{\hat{\beta}_{(0,0),h}\right\} \cup \{\beta_{\mathbf{i},h} : \mathbf{i} \in \mathbb{I}_h \backslash \mathbb{D}_1\}$$

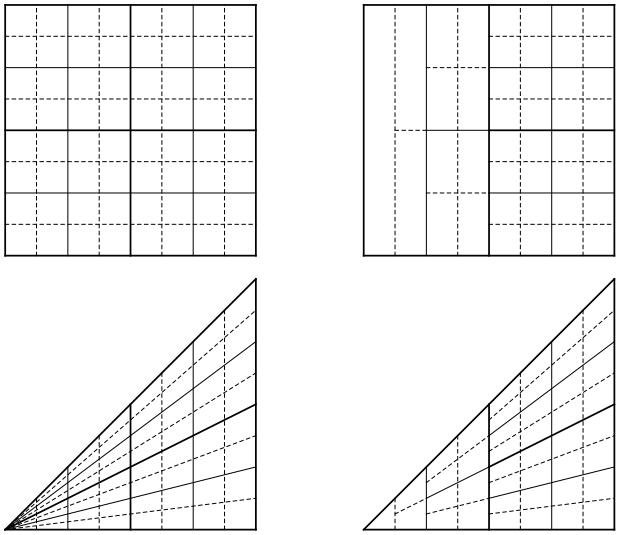

Figure 1: Triangle A with uniform (left) and adaptive (right) refinement

forms a partition of unity and all test functions are non-negative. We present a similar modification scheme for H^2 in Section 3.3.

Remark 3.4 *Note that the refinement is very crucial to the stability and approximation properties of the numerical method. Figure 1 shows two different refinement schemes. We point out various properties of the resulting meshes. The first example is a uniform refinement, splitting each knot interval in half in every step. The second example is a gradual refinement, refining less in a neighbourhood of the singularity. The goal of this refinement scheme is to keep the patches $\Delta \in \Lambda_h$ in the physical domain equally sized.*

Having a uniform refinement we get $\theta_\Delta = O(h)$ for all $\Delta \in \Lambda_h$, but $\min(\rho_\Delta) = O(h^2)$. Hence $\min(|\Delta|) = O(h^3)$ and $\max(|\Delta|) = O(h^2)$.

This can be avoided using adaptive refinement. The upper right image of Figure 1 presents a suitable scheme. For each level of refinement the non-uniform mesh is based on an underlying uniform mesh. We set the mesh size h of the non-uniform refinement to be the size of the underlying uniform mesh. The depicted refinement levels are $h = 1/2^0$ (whole domain), $h = 1/2^1$ (bold lines), $h = 1/2^2$ (thin lines) and $h = 1/2^3$ (dashed lines). Using this scheme we get $\theta_\Delta = O(h)$, $\rho_\Delta = O(h)$ and $|\Delta| = O(h^2)$ for all $\Delta \in \Lambda_h$.

The presented adaptive refinement scheme fulfills many desired properties. Apart from one patch, namely the one containing the singularity, all patches are regular quadrilaterals. We suppose that this scheme leads to a refined series of function spaces with very good stability and approximation properties. It is reasonable that this non-uniform refinement scheme can be applied to other domains of similar geometric structure.

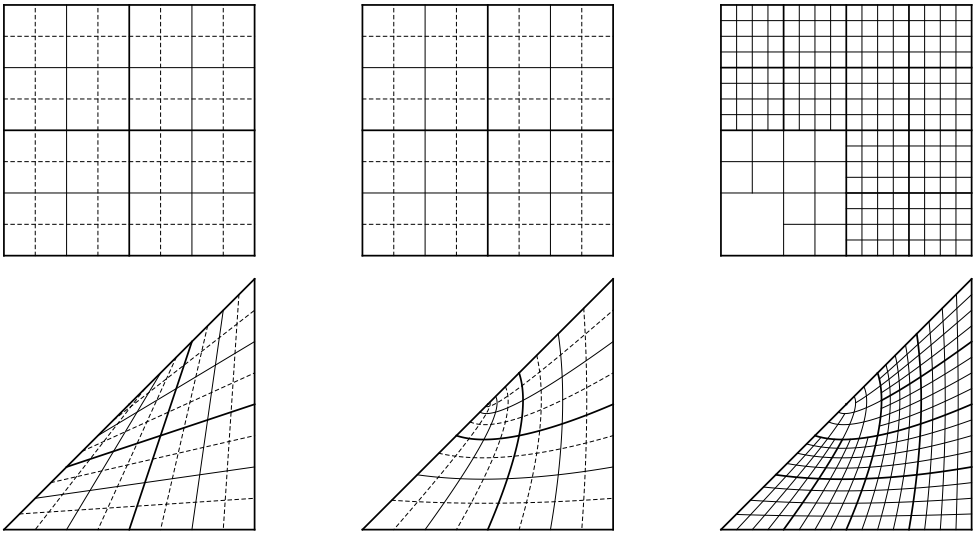

Figure 2: Triangle B1 with uniform refinement (left), Triangle B2 with uniform (middle) and adaptive (right) refinement

3.2 Triangles B1 and B2: Collinear edges

Similar to the results from the previous section we can derive regularity results for function spaces on the triangular domain Ω_B.

Theorem 3.5 *Consider the triangular domain Ω_B with parametrisation $\mathbf{G}_{B1}$ or $\mathbf{G}_{B2}$, respectively. Let $\mathbb{I}_h$ be the index set corresponding to an arbitrary refinement $\mathcal{D}_h$, with function space $\mathcal{V}_h$. We set*

$$\mathbb{D}_2 = \{(i,j) \in \mathbb{I}_h : i+j \leq 2\} \setminus \{(1,1)\}.$$

The test functions $\beta_{\mathbf{i},h}$ fulfill $\beta_{\mathbf{i},h} \in H^1(\Omega_B)$ for all $\mathbf{i} \in \mathbb{I}_h$ and $\beta_{\mathbf{i},h} \notin H^2(\Omega_B)$ if and only if $\mathbf{i} \in \mathbb{D}_2$.

Proof. For a proof of this theorem see [24, 25]. □

Remark 3.6 *We again want to consider different refinement strategies and compare the properties. We consider a uniform refinement for Triangles B1 and B2 and a specific local refinement for Triangle B2.*

For the uniform refinement of Triangle B1 (left) we get $\min(\theta_\Delta/\rho_\Delta) = O(1/h)$. Furtheron, $\min(|\Delta|) = O(h^3)$ and $\max(|\Delta|) = O(h^2)$. This means that, in any case, the shapes of the patches in the physical domain are degenerating. The depicted refinement levels for the uniform meshes in Figure 2 (left and middle) are $h = 1/2^0$ (whole domain), $h = 1/2^1$ (bold lines), $h = 1/2^2$ (thin lines) and $h = 1/2^3$ (dashed lines).

The uniform refinement of Triangle B2 (middle) leads to $\theta_\Delta/\rho_\Delta = O(1)$. This means that the shapes of the patches do not degenerate. But nevertheless, $\min(|\Delta|) = O(h^4)$ and $\max(|\Delta|) = O(h^2)$.

Patches with uniform area can be achieved using the presented adaptive refinement. The refinement levels for the rightmost pictures in Figure 2 are $h = 1/2^0$ (whole domain), $h = 1/2^2$ (bold lines) and $h = 1/2^4$ (thin lines). Hence, one refinement step of the non-uniform scheme is based on two steps of uniform refinement. Using this scheme we get $\theta_\Delta = O(h)$, $\rho_\Delta = O(h)$ and $|\Delta| = O(h^2)$ for all $\Delta \in \Lambda_h$.

Similar to the scheme presented for Triangle A, the adaptive refinement fulfills many desired properties. Again, all but one patches are regular quadrilaterals. Good stability and approximation properties can be assumed, also in the case of more general, geometrically similar domains.

3.3 Modification scheme for H^2

Having a singularly parametrised domain it might happen that $\mathcal{V}_h \not\subseteq H^2(\Omega)$. In the following proposition we present a scheme to compute a function space $\hat{\mathcal{V}}_h \subseteq \mathcal{V}_h \cap H^2(\Omega)$. This function space can then be used for numerical simulation where H^2-regularity is necessary.

Proposition 3.7 ([25]) *Consider a parametrisation*

$$\mathbf{G}(x,y) = (\xi_1, \xi_2) = \sum_{\mathbf{i} \in \mathbb{I}_h} \mathbf{P}_\mathbf{i}\, b_{\mathbf{i},h}(x,y)$$

where $\mathbf{P}_\mathbf{i} = (P_\mathbf{i}^1, P_\mathbf{i}^2)^T$ *are the control points. Let* $\mathbb{D}_2 \subseteq \mathbb{I}_h$ *be the set of all indices with* $\mathbf{i} \in \mathbb{D}_2$ *if and only if* $\beta_{\mathbf{i},h} \notin H^2(\Omega)$. *We define the function space* $\hat{\mathcal{V}}_h \subseteq \mathcal{V}_h$ *as the span of*

$$\begin{aligned}
\hat{\beta}_{(0,0),h}(\boldsymbol{\xi}) &= \sum_{\mathbf{i} \in \mathbb{D}_2} C_\mathbf{i}\ \beta_{\mathbf{i},h}(\boldsymbol{\xi}), \\
\hat{\beta}_{(1,0),h}(\boldsymbol{\xi}) &= \sum_{\mathbf{i} \in \mathbb{D}_2} \hat{P}_\mathbf{i}^1 / \hat{P}_{\max}\ \beta_{\mathbf{i},h}(\boldsymbol{\xi}), \\
\hat{\beta}_{(0,1),h}(\boldsymbol{\xi}) &= \sum_{\mathbf{i} \in \mathbb{D}_2} \hat{P}_\mathbf{i}^2 / \hat{P}_{\max}\ \beta_{\mathbf{i},h}(\boldsymbol{\xi}), \quad \textit{and} \\
\hat{\beta}_{\mathbf{i},h}(\boldsymbol{\xi}) &= \beta_{\mathbf{i},h}(\boldsymbol{\xi}) \quad \textit{for } \mathbf{i} \in \mathbb{I}_h \backslash \mathbb{D}_2,
\end{aligned}$$

where

$$\hat{P}_\mathbf{i}^k = \frac{P_\mathbf{i}^k - \min_{\mathbf{j} \in \mathbb{D}_2}\left(P_\mathbf{j}^k\right)}{\max_{\mathbf{j} \in \mathbb{D}_2}\left(P_\mathbf{j}^k\right) - \min_{\mathbf{j} \in \mathbb{D}_2}\left(P_\mathbf{j}^k\right)} \quad \textit{and} \quad C_\mathbf{i} = 1 - \frac{\hat{P}_\mathbf{i}^1 + \hat{P}_\mathbf{i}^2}{\hat{P}_{\max}}$$

with $\hat{P}_{\max} = \max_{\mathbf{j} \in \mathbb{D}_2}\left(\hat{P}_\mathbf{j}^1 + \hat{P}_\mathbf{j}^2\right)$. *For this space we obtain* $\hat{\mathcal{V}}_h \subseteq \mathcal{V}_h \cap H^2(\Omega)$.

Proof. This result is a direct consequence of the fact that

$$\sum_{\mathbf{i} \in \mathbb{I}_h} \hat{P}_\mathbf{i}^1\, \beta_{\mathbf{i},h}(\boldsymbol{\xi}) = \sum_{\mathbf{i} \in \mathbb{I}_h} \hat{P}_\mathbf{i}^1\, b_{\mathbf{i},h}\left(\mathbf{G}^{-1}(\boldsymbol{\xi})\right) = G^1\left(\mathbf{G}^{-1}(\boldsymbol{\xi})\right) = \xi_1 \in H^2(\Omega),$$

$$\sum_{\mathbf{i}\in\mathbb{I}_h} \hat{P}^2_{\mathbf{i}}\, \beta_{\mathbf{i},h}\left(\boldsymbol{\xi}\right) = G^2\left(\mathbf{G}^{-1}\left(\boldsymbol{\xi}\right)\right) = \xi_2 \in H^2\left(\Omega\right)$$

and

$$\sum_{\mathbf{i}\in\mathbb{I}_h} \beta_{\mathbf{i},h}\left(\boldsymbol{\xi}\right) = 1 \in H^2\left(\Omega\right);$$

and of the linearity of the function space $H^2\left(\Omega\right)$. □

This modification scheme generates a function space that fulfills the desired regularity condition $\hat{\mathcal{V}}_h \subseteq H^2\left(\Omega\right)$. The basis $\left\{\hat{\beta}_{\mathbf{j},h}\right\}$ forms a partition of unity and all basis functions are non-negative. Furtheron, the test functions $\hat{\beta}_{\mathbf{j},h}$ can be evaluated in a stable way. Hence the basis is suitable for numerical simulations.

4 Singular parametrisations of fillets

In this section we present four different fillet parametrisations. The first 3 parametrisations represent the same B-spline fillet patch. The fourth patch uses a quarter of a circle as fillet curve, hence the domain has a NURBS representation. The circular fillet patch is taken from [17].

Example 4.1 (Parabolic Fillet A.) *Let Ω be a Bézier patch having control points*

$\mathbf{P}_{(i,j)}$	$j=0$	$j=1$	$j=2$
$i=0$	$(0,0)^T$	$\left(\frac{1}{2},0\right)^T$	$\left(\frac{3}{4},\frac{1}{4}\right)^T$
$i=1$	$\left(\frac{7}{8},0\right)^T$	$\left(\frac{15}{16},\frac{1}{16}\right)^T$	$\left(1,\frac{1}{2}\right)^T$
$i=2$	$(1,0)^T$	$\left(1,\frac{1}{8}\right)^T$	$(1,1)^T$

as depicted in the top left of Figure 3. For this parametrisation the test functions fulfill $\beta_{\mathbf{i}} \in H^1\left(\Omega\right)$ and $\beta_{\mathbf{i}} \notin H^2\left(\Omega\right)$ for all **i**.

Example 4.2 (Parabolic Fillet B.) *Let Ω be a Bézier patch having control points*

$\mathbf{P}_{(i,j)}$	$j=0$	$j=1$	$j=2$
$i=0$	$(0,0)^T$	$\left(\frac{1}{2},0\right)^T$	$\left(\frac{3}{4},\frac{1}{4}\right)^T$
$i=1$	$\left(\frac{7}{8},0\right)^T$	$\left(\frac{7}{8},\frac{1}{8}\right)^T$	$\left(1,\frac{1}{2}\right)^T$
$i=2$	$(1,0)^T$	$\left(1,\frac{1}{8}\right)^T$	$(1,1)^T$

as in the top right of Figure 3. We have $\beta_{(i,j)} \notin H^1\left(\Omega\right)$ for $i+2-j \leq 1$, $\beta_{(i,j)} \in H^1\left(\Omega\right)$ for $i+2-j > 1$ and $\beta_{\mathbf{i}} \notin H^2\left(\Omega\right)$ for all **i**.

Example 4.3 (Parabolic Fillet C.) *Let Ω be a Bézier patch having control points*

$\mathbf{P}_{(i,j)}$	$j=0$	$j=1$	$j=2$
$i=0$	$(0,0)^T$	$\left(\frac{1}{2},0\right)^T$	$\left(\frac{3}{4},\frac{1}{4}\right)^T$
$i=1$	$\left(\frac{1}{2},0\right)^T$	$\left(\frac{7}{8},\frac{1}{8}\right)^T$	$\left(1,\frac{1}{2}\right)^T$
$i=2$	$(1,0)^T$	$\left(1,\frac{1}{2}\right)^T$	$(1,1)^T$

as in the bottom left of Figure 3. We have $\beta_{\mathbf{i}} \notin H^1(\Omega)$ *for* $\mathbf{i} \neq (2,0)$ *and* $\beta_{\mathbf{i}} \in H^2(\Omega)$ *for* $\mathbf{i} = (2,0)$.

Example 4.4 (Circular Fillet [17].) *Let* Ω_C *be a NURBS patch having control points*

$\mathbf{P}_{(i,j)}$	$j=0$	$j=1$	$j=2$
$i=0$	$(0,0)^T$	$\left(\sqrt{2}-1,0\right)^T$	$\left(\frac{1}{\sqrt{2}},1-\frac{1}{\sqrt{2}}\right)^T$
$i=1$	$\left(\frac{17}{20},0\right)^T$	$\left(\frac{17}{20},\frac{3}{20}\right)^T$	$\left(1,2-\sqrt{2}\right)^T$
$i=2$	$(1,0)^T$	$\left(1,\frac{3}{20}\right)^T$	$(1,1)^T$

and weigths

$\omega_{(i,j)}$	$j=0$	$j=1$	$j=2$
$i=0$	1	$\cos\left(\frac{\pi}{8}\right)$	1
$i=1$	1	1	$\cos\left(\frac{\pi}{8}\right)$
$i=2$	1	1	$1.$

The control points and parametrisation are depicted at the bottom right of Figure 3. The NURBS test functions are defined as

$$r_{\mathbf{i}}(\mathbf{x}) = \frac{\omega_{\mathbf{i}} b_{\mathbf{i}}(\mathbf{x})}{\sum_{\mathbf{j}} \omega_{\mathbf{j}} b_{\mathbf{j}}(\mathbf{x})}$$

and $\mathbf{G}(\mathbf{x}) = \sum_{\mathbf{i}} \mathbf{P}_{\mathbf{i}} r_{\mathbf{i}}(\mathbf{x})$. *Similar to the parabolic fillet A all test functions fulfill* $\rho_{\mathbf{i}} = r_{\mathbf{i}} \circ \mathbf{G}^{-1} \in H^1(\Omega_C)$ *and* $\rho_{\mathbf{i}} \notin H^2(\Omega_C)$.

Figure 3 gives an overview of the four fillet patches. Test functions $\beta_{\mathbf{i}}$ corresponding to control points $\mathbf{P}_{\mathbf{i}}$ depicted in blue fulfill $\beta_{\mathbf{i}} \in H^2$, test functions corresponding to control points depicted in green fulfill $\beta_{\mathbf{i}} \notin H^2$ and $\beta_{\mathbf{i}} \in H^1$; and test functions corresponding to control points depicted in red fulfill $\beta_{\mathbf{i}} \notin H^1$. All the results can be proven in the same manner as the results for triangular patches. We will not present the proofs here.

The control point grids for fillets A and B are equal, with the only exception that the inner control points differ. Surprisingly, the regularity properties of the test functions differ. This is due to the fact that the fillet B represents a limit case. If the inner control point would be even closer to the singularity at $\boldsymbol{\xi} = (3/4, 1/4)^T$, then the parametrisation would fold over. Hence the singularity is of a higher order. Fillet C is also similar to fillets A and B, but in that case also the control points on the straight line boundaries are changed. This does not affect the geometry, but the regularity of the test function space is reduced.

5 Conclusion

We presented H^1 and H^2 regularity results for the test functions from isogeometric analysis in the presence of singularities in the parametrisation. We considered triangular domains and fillet patches. It is necessary to point out that similar results can be

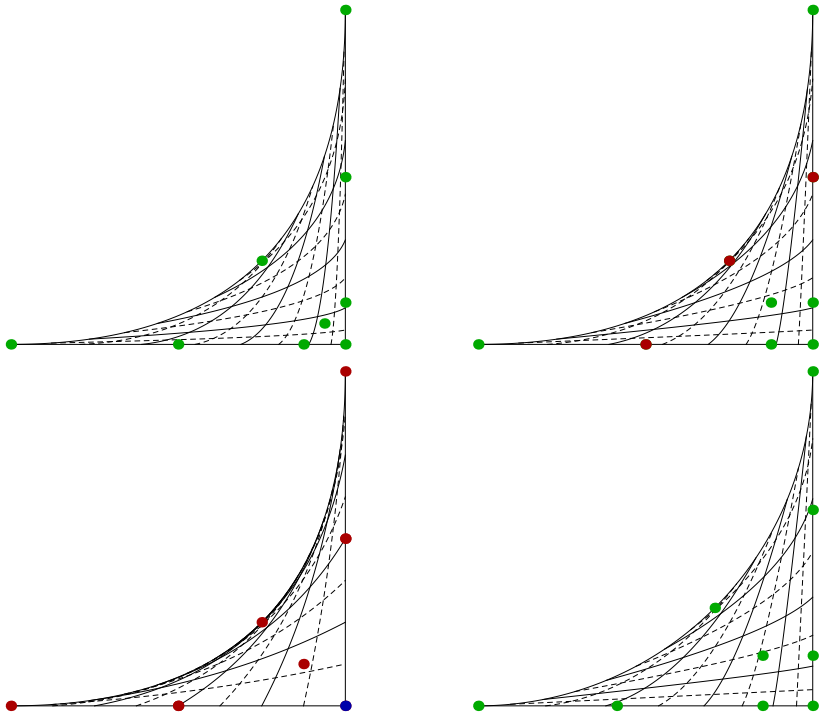

Figure 3: Parabolic fillets A (top left), B (top right) and C (bottom left) and circular fillet (bottom right)

achieved for more general domains. We also presented modification schemes for the test function space in case of reduced regularity. The schemes reproduce test functions that are in H^1 or H^2, respectively, generating function spaces suitable for numerical analysis.

Using the example of a triangular domain we presented different parametrisation strategies and refinement schemes. We suppose that specific local refinement strategies combined with the H^2 modification scheme seem to be a strong tool to achieve good numerical results for singularly parametrised domains. This needs to be confirmed by numerical simulations of real-world problems.

As we presented in the case of fillet patches, the choice of the inner control points and the boundary representation might have an effect on the regularity properties of the test functions. Negative effects, like reduced regularity, high instability or weak approximation order, can lead to bad simulation results. These effects need to be studied in more detail. Our findings suggest that a careful treatment of singularities is necessary in many cases. But, if done properly, it leads to a very convenient method for numerical simulation on very general physical domains.

Acknowledgements

This research was partially supported by the Austrian Science Fund (FWF): W1214-N15, project DK3.

References

[1] Y. Bazilevs, V. M. Calo, J. A. Cottrell, J. A. Evans, T. J. R. Hughes, S. Lipton, M. A. Scott, and T. W. Sederberg. Isogeometric analysis using T-splines. *Computer Methods in Applied Mechanics and Engineering*, 199(5-8):229 – 263, 2010.

[2] Y. Bazilevs, L. Beirão da Veiga, J. A. Cottrell, T. J. R. Hughes, and G. Sangalli. Isogeometric analysis: approximation, stability and error estimates for h-refined meshes. *Mathematical Models and Methods in Applied Sciences*, 16(7):1031 – 1090, 2006.

[3] S. Brenner and R. L. Scott. *The Mathematical Theory of Finite Element Methods*. Springer, 2005.

[4] A. Buffa, G. Sangalli, and R. Vázquez. Isogeometric analysis in electromagnetics: B-splines approximation. *Computer Methods in Applied Mechanics and Engineering*, 199(17-20):1143 – 1152, 2010.

[5] E. Cohen, T. Martin, R. M. Kirby, T. Lyche, and R. F. Riesenfeld. Analysis-aware modeling: Understanding quality considerations in modeling for isogeometric analysis. *Computer Methods in Applied Mechanics and Engineering*, 199(5-8):334 – 356, 2010.

[6] J. A. Cottrell, T. J. R. Hughes, and A. Reali. Studies of refinement and continuity in isogeometric structural analysis. *Computer Methods in Applied Mechanics and Engineering*, 196(41-44):4160 – 4183, 2007.

[7] J. A. Cottrell, A. Reali, Y. Bazilevs, and T. J. R. Hughes. Isogeometric analysis of structural vibrations. *Computer Methods in Applied Mechanics and Engineering*, 195(41-43):5257 – 5296, 2006.

[8] M. R. Dörfel, B. Jüttler, and B. Simeon. Adaptive isogeometric analysis by local h-refinement with T-splines. *Computer Methods in Applied Mechanics and Engineering*, 199(5-8):264 – 275, 2010.

[9] Tor Dokken, Tom Lyche, and Kjell Fredrik Pettersen. Locally refinable splines over box-partitions. Technical report, SINTEF, 2012.

[10] David R. Forsey and Richard H. Bartels. Hierarchical B-spline refinement. *SIGGRAPH Comput. Graph.*, 22(4):205–212, jun 1988.

[11] Carlotta Giannelli, Bert Jüttler, and Hendrik Speleers. THB-splines: The truncated basis for hierarchical splines. *Computer Aided Geometric Design*, (0):–, 2012.

[12] Klaus Höllig, Ulrich Reif, and Joachim Wipper. Weighted extended B-spline approximation of dirichlet problems. *SIAM Journal on Numerical Analysis*, 39(2):442–462, 2001.

[13] T. J. R. Hughes, J. A. Cottrell, and Y. Bazilevs. Isogeometric analysis: CAD, finite elements, NURBS, exact geometry and mesh refinement. *Computer Methods in Applied Mechanics and Engineering*, 194(39-41):4135 – 4195, 2005.

[14] J. Kiendl, Y. Bazilevs, M.-C. Hsu, R. Wüchner, and K.-U. Bletzinger. The bending strip method for isogeometric analysis of Kirchhoff-Love shell structures comprised of multiple patches. *Computer Methods in Applied Mechanics and Engineering*, 199(37-40):2403 – 2416, 2010.

[15] Hyun-Jung Kim, Yu-Deok Seo, and Sung-Kie Youn. Isogeometric analysis with trimming technique for problems of arbitrary complex topology. *Computer Methods in Applied Mechanics and Engineering*, 199(45-48):2796 – 2812, 2010.

[16] Stefan K. Kleiss, Bert Jüttler, and Walter Zulehner. Enhancing isogeometric analysis by a finite element-based local refinement strategy. *Computer Methods in Applied Mechanics and Engineering*, 213-216(0):168 – 182, 2012.

[17] S. Lipton, J. A. Evans, Y. Bazilevs, T. Elguedj, and T. J. R. Hughes. Robustness of isogeometric structural discretizations under severe mesh distortion. *Computer Methods in Applied Mechanics and Engineering*, 199(5-8):357 – 373, 2010.

[18] J. Lu. Circular element: Isogeometric elements of smooth boundary. *Computer Methods in Applied Mechanics and Engineering*, 198(30-32):2391 – 2402, 2009.

[19] T. Martin, E. Cohen, and R. M. Kirby. Volumetric parameterization and trivariate B-spline fitting using harmonic functions. *Computer Aided Geometric Design*, 26(6):648 – 664, 2009.

[20] L. Piegl and W. Tiller. *The NURBS book*. Springer, London, 1995.

[21] H. Prautzsch, W. Boehm, and M. Paluszny. *Bézier and B-Spline Techniques*. Springer, New York, 2002.

[22] L. L. Schumaker. *Spline Functions: Basic Theory*. Cambridge University Press, Cambridge, 2007.

[23] T. W. Sederberg, J. Zheng, A. Bakenov, and A. Nasri. T-splines and T-NURCCS. *ACM Transactions on Graphics*, 22(3):477 – 484, 2003.

[24] T. Takacs and B. Jüttler. Existence of stiffness matrix integrals for singularly parameterized domains in isogeometric analysis. *Computer Methods in Applied Mechanics and Engineering*, 200(49-52):3568 – 3582, 2011.

[25] Thomas Takacs and Bert Jüttler. H^2 regularity properties of singular parameterizations in isogeometric analysis. *Graphical Models*, 2011. in-press.

[26] Y. Zhang, Y. Bazilevs, S. Goswami, C. L. Bajaj, and T. J. R. Hughes. Patient-specific vascular NURBS modeling for isogeometric analysis of blood flow. *Computer Methods in Applied Mechanics and Engineering*, 196(29-30):2943 – 2959, 2007.